

Video Article

# Fluorescence-quenching of a Liposomal-encapsulated Near-infrared Fluorophore as a Tool for *In Vivo* Optical Imaging

Felista L. Tansi<sup>\*1</sup>, Ronny Rüger<sup>\*2</sup>, Markus Rabenhold<sup>2</sup>, Frank Steiniger<sup>3</sup>, Alfred Fahr<sup>2</sup>, Ingrid Hilger<sup>1</sup>

<sup>1</sup>Experimental Radiology, Institute of Diagnostic and Interventional Radiology I, Jena University Hospital

<sup>2</sup>Department of Pharmaceutical Technology, Friedrich-Schiller-University Jena

<sup>3</sup>Center for Electron Microscopy, Jena University Hospital

\*These authors contributed equally

Correspondence to: Felista L. Tansi at [Felista.Tansi@med.uni-jena.de](mailto:Felista.Tansi@med.uni-jena.de), Ronny Rüger at [ronny.rueger@uni-jena.de](mailto:ronny.rueger@uni-jena.de), Ingrid Hilger at [ingrid.hilger@med.uni-jena.de](mailto:ingrid.hilger@med.uni-jena.de)

URL: <https://www.jove.com/video/52136>

DOI: [doi:10.3791/52136](https://doi.org/10.3791/52136)

Keywords: Bioengineering, Issue 95, Drug-delivery, Liposomes, Fluorochromes, Fluorescence-quenching, Optical imaging, Inflammation

Date Published: 1/5/2015

Citation: Tansi, F.L., Rüger, R., Rabenhold, M., Steiniger, F., Fahr, A., Hilger, I. Fluorescence-quenching of a Liposomal-encapsulated Near-infrared Fluorophore as a Tool for *In Vivo* Optical Imaging. *J. Vis. Exp.* (95), e52136, doi:10.3791/52136 (2015).

## Abstract

Optical imaging offers a wide range of diagnostic modalities and has attracted a lot of interest as a tool for biomedical imaging. Despite the enormous number of imaging techniques currently available and the progress in instrumentation, there is still a need for highly sensitive probes that are suitable for *in vivo* imaging. One typical problem of available preclinical fluorescent probes is their rapid clearance *in vivo*, which reduces their imaging sensitivity. To circumvent rapid clearance, increase number of dye molecules at the target site, and thereby reduce background autofluorescence, encapsulation of the near-infrared fluorescent dye, DY-676-COOH in liposomes and verification of its potential for *in vivo* imaging of inflammation was done. DY-676 is known for its ability to self-quench at high concentrations. We first determined the concentration suitable for self-quenching, and then encapsulated this quenching concentration into the aqueous interior of PEGylated liposomes. To substantiate the quenching and activation potential of the liposomes we use a harsh freezing method which leads to damage of liposomal membranes without affecting the encapsulated dye. The liposomes characterized by a high level of fluorescence quenching were termed Lip-Q. We show by experiments with different cell lines that uptake of Lip-Q is predominantly by phagocytosis which in turn enabled the characterization of its potential as a tool for *in vivo* imaging of inflammation in mice models. Furthermore, we use a zymosan-induced edema model in mice to substantiate the potential of Lip-Q in optical imaging of inflammation *in vivo*. Considering possible uptake due to inflammation-induced enhanced permeability and retention (EPR) effect, an always-on liposome formulation with low, non-quenched concentration of DY-676-COOH (termed Lip-Q) and the free DY-676-COOH were compared with Lip-Q in animal trials.

## Video Link

The video component of this article can be found at <https://www.jove.com/video/52136/>

## Introduction

Liposomes have been intensively investigated and serve as one of the most biocompatible biomedical drug delivery systems for clinical applications<sup>1,2</sup>. They are mainly composed of phospholipids and cholesterol, both of which are biocompatible compounds mimicking parts of natural cell membranes. Whereas hydrophilic substances can be entrapped in the aqueous interior, lipophilic agents can be incorporated within the liposomal phospholipid bilayer<sup>3</sup>. Encapsulation of substances within the aqueous interior of liposomes grants protection against degradation *in vivo* and also prevents the host system from toxic effects of cytotoxic drugs used for the therapy of diseases, for example chemotherapeutics aimed at destroying tumor cells. The modification of the liposomal surface with polymers like polyethylenglycol (PEGylation) further extends the liposomal blood circulation time *in vivo* due to sterical stabilization<sup>4</sup>. Moreover, liposomes can sequester high concentrations of several substances such as proteins<sup>5,6</sup>, hydrophilic substances<sup>7,8</sup> and enzymes<sup>9</sup>. They therefore serve as reliable clinical therapeutic and diagnostic tools which merit their approval for delivery of cytotoxic drugs such as doxorubicin for cancer therapy<sup>4</sup>. Due to their flexibility, liposomes can also be loaded with fluorochromes for diagnostic and image-guided surgical purposes.

Fluorescence imaging provides a cost-effective and non-invasive *in vivo* diagnostic tool which however, demands some basic requirements. It could be demonstrated that fluorochromes which suit best for *in vivo* imaging have characteristic absorption and emission maxima in the range where light dispersion and scattering as well as tissue autofluorescence originating from water and hemoglobin is low. Thus, such probes have their abs/em maxima between 650 and 900 nm<sup>10</sup>. Besides this, the stability of fluorochromes both *in vitro* and *in vivo* is critical, as opsonization and rapid clearance can greatly limit their application for *in vivo* imaging<sup>11</sup>. Other effects such as poor stability and low sensitivity or cytotoxic effects on target organs as seen with indocyanine green (ICG)<sup>12-16</sup>, are unwanted and must be taken into consideration when designing probes for *in vivo* imaging. These observations have led to the active development of several preclinical NIR fluorochromes, nanoparticles as well as new techniques for the *in vivo* imaging of inflammatory processes, cancer and for image-guided surgery<sup>17-20</sup>. Despite the stability of most

preclinical NIRF (near-infrared fluorescence) dyes *in vitro*, their rapid perfusion and clearance through the liver and kidney impede their use in the *in vivo* optical imaging of diseases and inflammatory processes.

We therefore present a protocol for the encapsulation of fluorochromes such as the well characterized near-infrared fluorescent dye DY-676-COOH, known for its tendency to self-quench at relatively high concentrations<sup>21</sup> in liposomes. At high concentrations H-dimer formation and/or pi-stacking interactions between fluorophore molecules located within each other's Förster radius result in Förster resonance energy transfer (FRET) between the fluorochrome molecules. At low concentration the space between the fluorophore molecules increases, thereby preventing pi-stacking interaction and H-dimer formation and resulting in high fluorescence emission. The switch between high and low concentration and the accompanying fluorescence quenching and activation is a promising strategy that can be exploited for optical imaging<sup>22</sup>. In this respect, encapsulation of high concentrations of the NIRF dye DY-676-COOH in the aqueous interior of liposomes is more favorable for *in vivo* imaging than the free dye. The challenge of the method lies first of all in the correct encapsulation and secondly, in the validation of the benefits resulting from encapsulating high concentrations of the dye. Comparing the imaging properties of quenched liposomes with that of the free dye and also with a non-quenched liposome formulation with low concentrations of the dye is indispensable. We show by a simple, but highly effective film hydration and extrusion protocol combined with alternate freeze and thaw cycles that encapsulation of quenching concentrations of DY-676-COOH in liposomes is feasible. Other methods used to prepare liposomes such as the reversed phase evaporation method<sup>23</sup> as well as the ethanol injection method<sup>24</sup> enable liposome preparation with high encapsulation efficiencies for many hydrophilic substances. However, the nature of the substance to be encapsulated can influence the encapsulation efficiency. In effect, the film hydration and extrusion protocol presented here revealed the highest efficiency for encapsulation of DY-676-COOH. To illustrate the benefits of liposomal encapsulation of DY-676-COOH, a zymosan-induced edema model, which permits the study of inflammatory processes within a few hours, was used. Here, it is demonstrated that liposomes with high concentrations of the encapsulated DY-676-COOH are more suitable for whole body *in vivo* optical imaging of inflammatory processes than the free dye or the non-quenched liposomal formulation with low dye concentrations. Thus the underlying protocol provides a simple and fast method to produce quenched fluorescent liposomes and the validation of their activation and imaging potential both *in vitro* and *in vivo*.

## Protocol

NOTE: All procedures are approved by the regional animal committee and in accordance with international guidelines on the ethical use of animals.

## 1. Preparation of Materials and Instruments

- Preparation of spontaneously formed vesicle dispersion (SFV)
  - Dissolve and prepare stock solutions of the following phospholipids: 214 mg/ml egg phosphatidylcholine (EPC), 134 mg/ml cholesterol, 122 mg/ml 1,2-distearoyl-*sn*-glycero-3-phosphoethanolamine-*N*-[methoxy(polyethylene glycol)-2000] (ammonium salt) (mPEG<sub>2000</sub>-DSPE) and 2 mg/ml 1,2-dioleoyl-*sn*-glycero-3-phosphoethanolamine-*N*-(7-nitro-2-1,3-benzoxadiazol-4-yl) (ammonium salt) (NBD-DOPE) in chloroform and store in glass vials.
  - Furnish approximately 3 ml chloroform in a round bottom flask and transfer the appropriate volume of phospholipid stock solution into the round bottom flask to prepare liposomes composed of EPC:Chol:mPEG<sub>2000</sub>-DSPE at a molar ratio of 6.5:3:0.5. For double fluorescence labeling of liposomes add 0.3 mol% NBD-DOPE to the lipid solution.
  - Evaporate the chloroform from the organic phospholipid solution under reduced pressure (300 mbar) at 55 °C using a rotary evaporator.
  - After a homogeneous phospholipid film is formed, reduce the pressure to 10 mbar for 1-2 hr to remove residual chloroform deposit.
  - While the chloroform is evaporating, dissolve DY-676-COOH (6.181 µM) in 10 mM Tris buffer pH 7.4 and fill a Dewar vessel with liquid nitrogen. Switch on an ultrasonic bath and set at 50 °C.
  - Transfer an appropriate volume (0.5–1 ml) of DY-676-COOH (6.181 µM) solution to the round bottom flask to hydrate the dry phospholipid film and vortex vigorously until a spontaneously formed vesicle (SFV) dispersion forms. Make sure that all of the phospholipids are dispersed to avoid lipid loss.
  - Carefully transfer the round bottom flask containing the SFV dispersion into liquid nitrogen and freeze the dispersion for 3–5 min. Place the round bottom flask into an ultrasonic bath at 50 °C to thaw the dispersion then vortex the dispersion vigorously for 1–2 min. Repeat this procedure six times, making a total of seven freeze and thaw cycles.
- Extrusion of SFV to form homogeneous liposome vesicles
  - Transfer the SFV dispersion into a 1 ml syringe (syringe-a) and extrude the dispersion through a 100 nm polycarbonate membrane using a LiposoFast-Basic extruder into syringe-b.
  - Extrude the dispersion from syringe-b, back into syringe-a, then repeat the cycle ten times. Due to extrusion, the solution in the syringe changes from a hazy appearance to a clear dispersion with time. After ten cycles (twenty single extrusion steps) remove syringe-b from the device and extrude the dispersion for the last time from syringe-a directly into a sterile 1.5 ml reaction tube.
- Purification of liposomal encapsulated DY-676-COOH from free dye
  - Prepare a gel chromatography column using G25 beads soaked in 10 mM Tris buffer pH 7.4 (column length 28 cm, diameter 0.8 cm).
  - Transfer 0.5 ml of extruded vesicle dispersion onto the gel bed and let the sample drain into the gel matrix.
  - Elute the liposomes with 10 mM Tris buffer pH 7.4 (**Figure 1A**) and wash the column until the free dye drains completely out of the column. If need be, collect and recycle the free dye by desalting and dehydration according to the manufacturer's instructions.
  - Concentrate the eluted liposomes by ultracentrifugation (200,000 x g, 2 hr at 8 °C) then disperse them in adequate volume of sterile 10 mM Tris buffer pH, 7.4.
- Quantification of encapsulated DY-676-COOH concentration
  - Prepare a calibration curve by dissolving DY-676-COOH (0, 82, 124, 247, 494, 988 nM) in 10 mM Tris buffer, pH 7.4 containing 0.1% Triton X100.

2. Dissolve 2  $\mu$ l (100 nmol final lipid of a 50 mmol/L stock) of the liposomes for 5 min at room temperature in 100  $\mu$ l Tris buffer containing 1% Triton X100 to destroy the vesicles and release the encapsulated dye. Then dilute samples with 10 mM Tris buffer, pH 7.4 to a final Triton-X100 concentration of 0.1% (v/v) making a total volume of 1 ml. Prepare all samples in duplicate.
3. Measure the absorption and emission of all samples (free DY-676-COOH and Triton-X100 treated liposomes) at an excitation  $\lambda$ =645 nm and an emission  $\lambda$  = 700 nm. Establish and use a calibration curve of the free dye to determine the concentration of encapsulated dye.
5. Liposome characterization
  1. Determine the sizes and zeta potential of liposomes by dynamic light scattering. Dilute the liposomal samples with filter sterilized (0.2  $\mu$ m) 10 mM Tris buffer pH 7.4 to a concentration of 100–300  $\mu$ M (lipid). Transfer the diluted samples into a low volume disposable cuvette and measure the sample according to the manufacturer's instructions.
  2. Characterize the liposomes by electron microscopy to substantiate the size, integrity and homogeneity of liposomal vesicles according to standard protocols.

## 2. Validation of Fluorescence-quenching and Activation of Prepared Liposomes

1. Physicochemical analysis of fluorescence quenching and activation
  1. Prepare two 1.5 ml tubes for the Lip-Q and 2 tubes for the free DY-676-COOH. Transfer 100 nmol total lipids (2.38  $\mu$ l of a 42 mmol/L Lip-Q stock solution, containing 138  $\mu$ g/ml of the encapsulated DY-676-COOH) into the corresponding tubes. Transfer free DY-676-COOH equivalent to the dye content of Lip-Q (0.38  $\mu$ g which results for example from 138  $\mu$ g/1,000  $\mu$ l x 2.38  $\mu$ l Lip-Q used). Incubate one tube of each probe at 4 °C and freeze the second tube at -80 °C overnight (16 hr).
  2. Heat up a heating block to 30 °C. Fill a cooling box with crushed ice and equilibrate an aliquot of 10 mM Tris buffer pH 7.4 to room temperature.
  3. Remove probes from 4 °C and equilibrate at room temperature (wrapped in aluminum foil to protect from light) and quickly thaw probes from -80 °C at 30 °C for 5 min. Chill the thawed probes on ice for 1 min before transferring them to room temperature (also wrapped in aluminum foil to protect from light).
  4. Add 10 mM Tris buffer (pH 7.4) to each of the probes to 100  $\mu$ l final volume and equilibrate all probes at RT for 10 min.
  5. Pipette 80  $\mu$ l of each probe into a low volume glass cuvette and measure the absorption of each probe from 400–900 nm on a spectrometer. Return the probe to their corresponding tubes.
  6. Transfer 80  $\mu$ l of each probe into a suitable glass cuvette and measure the fluorescence emission on a spectrofluorometer by exciting the probes at 674 nm and measuring the fluorescence from 694–800 nm.
2. Cellular uptake and fluorescence activation
  1. Get and culture the following cell lines in their corresponding culture media according to standard conditions (37 °C, 5% CO<sub>2</sub> and 95% humidified atmosphere). Here, use the murine macrophage cell line J774A.1 (Dulbecco's modified Eagle's medium supplemented with 10% (v/v) fetal calf serum), the human glioblastoma cell line, U-118MG (MEM containing essential vitamins and 10% (v/v) fetal calf serum) and the human fibrosarcoma cell line, HT-1080 (RPMI with 5% FCS).
  2. Coat 8-well chamber slides with poly-L-lysine (add 100  $\mu$ l 0.001% poly-L-lysine to each well and incubate at 37 °C for 10 min. Aspirate solution and let the chamber slides to dry up for at least 4 hr at RT on a sterile workbench. Rinse the chamber slides 3 times with 200  $\mu$ l Hank's buffered saline solution then seal them with paraffin and aluminum foil and store at 4 °C till needed.
  3. While the chamber slides are drying up, filter-sterilize the liposomes and dye solution and store at 4 °C till needed.
  4. For probe uptake analysis with the whole body *in vivo* NIR fluorescence imaging system, prepare 5 small culture flasks for each of the 3 test cell lines (15 flasks in total). Seed  $2 \times 10^6$  J774A.1, U-118MG and HT-1080 cells per culture flask with 5 ml of the respective culture medium (in quintuples) and grow for 16-24 hr. Parallel to the culture flasks, seed 30,000 cells of each cell line (J774A.1 and HT-1080) or 20,000 cells (U-118MG) to 2 wells of the chamber slide respectively and grow in 500  $\mu$ l culture medium for 16-24 hr.
  5. On the next day, add 100 nmol (final lipid amount) of Lip-Q to 2 flasks per cell line and to one well of each cell line on the chamber slide. Immediately transfer 1 flask per cell line to 4 °C and the second flask back to the incubator.  
NOTE: The volume of the probes added to the flasks and the chamber slides are the same, making the concentration on chamber slides 10-fold higher (5 ml is to 500  $\mu$ l culture medium). This is necessary because microscopic detection is less sensitive than the NIR fluorescence imaging system where cell pellets from the flasks are imaged.
  6. Add the free DY-676-COOH at a concentration equivalent to the dye content of Lip-Q to the cells in 2 flasks per cell line and to one well of each cell line on the chamber slide, then immediately transfer 1 flask per cell line to 4 °C (energy depletion) and the other flask together with the chamber slide back to the incubator. Incubate all the cells for 24 hr at the corresponding conditions. The cells in the flask without probe serve as untreated control.
3. NIRF imaging and semi-quantitative analysis
  1. After 24 hr incubation duration, harvest the cells in flasks by washing cells 2 times with Hanks buffered salt solution (HBSS) then scrape cells in 500  $\mu$ l HBSS and pellet by centrifugation (5 min at 200 x g) in 500  $\mu$ l tubes.
  2. Place the tubes with the cell pellets (and HBSS) in a NIRF imager and image using filters for excitation (615–665 nm) and emission (cut in >700 nm).
  3. Deduct autofluorescence and evaluate the intensity of target versus autofluorescence according to manufacturer instructions. This will give the semi-quantitative levels of fluorescence intensity as average signal (scaled counts/sec), which represents count levels after scaling for exposure time, camera gain, binning and bit depth, so that the measurements are comparable among each other.
4. Confocal microscopic analysis
  1. After 24 hr incubation, harvest the cells on chamber slides by washing 2 times with 500  $\mu$ l HBSS.
  2. Fix the cells with 200  $\mu$ l HBSS containing 3.7% (v/v) formaldehyde for 30 min at RT.
  3. While fixation is going on, dilute the DNA stain, Hoechst-33258 1:50 with mounting solution.

4. After fixation, wash the cells 2 times with HBSS then separate the chambers from the glass slides. Add 50  $\mu$ l mounting solution containing the DNA-stain on each spot corresponding to the wells of the chamber slides. Cover the cells with glass coverslips, seal edges with transparent nail polish and air-dry for 10 min at RT (dark).
  5. Image cells on a suitable fluorescence microscope or confocal microscope. Use the following excitation and emission settings for visualization of the corresponding components: nuclei (Hoechst-33258: excitation 405 nm, emission 420–480 nm). NBD-DOPE (liposomal lipid: excitation 488 nm, emission 530 nm). DY-676-COOH (NIR fluorescent dye: excitation 633–645 nm, emission 650–700 nm).
- NOTE: Make sure that the fluorescence microscope available is equipped with suitable filters which permit excitation and emission of wavelengths higher than 630 nm.

### 3. Liposome-based *In Vivo* Fluorescence Imaging of Inflammation

1. Preparation of animals and materials
  1. House 8–12 week-old male NMRI mice weighing approximately 36 g under standard conditions with food and water *ad libitum*.
  2. Seven days prior to the start of experiments, give all mice a low pheophorbide diet in order to reduce tissue autofluorescence.
  3. Twenty-four hours before the start of each experiment, shave mice at the desired area (e.g., whole back area if imaging of hind leg edema is desired).
  4. Weigh the animals and calculate the amount of probe to be injected per mouse (Lip-Q and Lip-dQ at 10  $\mu$ mol (lipid concentration) per kg weight and free DY-676-COOH (equivalent to dye content of Lip-Q used).
  5. Image the animals in a whole body NIR Fluorescence imager with the same settings used for the cell pellets. This measurement provides autofluorescence of the animals.
  6. Dissolve 10 mg zymosan-A in 1 ml isotonic saline solution and store overnight at 4 °C.
2. Induction of inflammation and *in vivo* NIRF imaging
  1. Prepare 3 syringes per mouse containing the following solutions. Fill one syringe with 50  $\mu$ l zymosan-A solution (10 mg/ml) and the second syringe with 50  $\mu$ l isotonic saline solution. Fill the third syringe with the probes, whereby Lip-Q and Lip-dQ (10  $\mu$ mol/kg weight (lipid)) are designated for test animals and free DY-676-COOH (concentration as in Lip-Q) for control animals. Make sure the probes are diluted with sterile HBSS to 150  $\mu$ l final volume.
  2. Apply eye cream on the eyes of animals to avoid dryness and anesthetize animals with 2% isoflurane till they are deeply asleep and do not react when touched on the paws (this takes about 2 min).
  3. Place the mouse on a warm mat (still under anesthesia) and inject the zymosan-A solution subcutaneously on the right hind leg and the saline solution on the left hind leg. Immediately inject the probe intravenously and image the animal thereafter then record time of injection/measurement (as  $t = 0$  hr). Save the resulting images as image cubes and repeat the above steps for all other animals and respective probes.
  4. Image the animals every 2 hr for 10 hr post injection and then at 24 hr post injection, making sure that the stage of the measuring chamber is warm (for example, by placing a warm mat underneath), in order to avoid hypothermia. After each measurement, place the animals in a cage with food and water *ad libitum* and place the cage in a temperate animal chamber. Euthanize the animals by first anesthetizing with 2% isoflurane till the animals no longer react to touch, then euthanize with carbon dioxide for 5–10 min, making sure that the animals stop breathing completely and rigor mortis occurs.
  5. Dissect the mice according to standard protocols which can be assessed online (<http://www.freebookez.com/mouse-dissection-lab-report/>) and image the organs.
  6. Evaluate the measurement results according to manufacturer's instructions by first deducting the overall fluorescence of the animals (unmixing) then assigning regions of interest for autofluorescence (left hind leg with saline) and target fluorescence of inflamed area (right hind leg with zymosan-A).

### Representative Results

The encapsulation of high concentrations of fluorescent dyes such as the NIRF dye DY676-COOH used here in the aqueous interior of liposomes leads to a high level of fluorescence quenching. Fluorescence quenching, a phenomenon seen with many fluorophores at high concentration, can be exploited in several *in vivo* imaging applications where a high sensitivity and reliable detection of the target area are demanded. The use of liposomes also provides protection of the dye which is indispensable for *in vivo* applications. A thorough characterization of the liposomes is necessary and includes several factors such as the level of dye encapsulated, stability and size of the liposomes, fluorescence quenching and activity of encapsulated dye *in vitro* and also applicability for *in vivo* imaging purposes. A comparison of the free dye, DY-676-COOH and quenched liposomes (Lip-Q) as well as a non-quenched liposome (Lip-dQ) with very low concentration of the encapsulated dye is therefore critical especially for *in vivo* characterizations.

Liposomes prepared by using the film hydration and extrusion technique with successive freeze and thaw cycles before extrusion contain residual free dye molecules which can be successfully separated from the liposomes due to their longer retention in the gel filtration matrix, compared to the liposomes which elute faster (**Figure 1B**). Depending on the level of dilution after gel filtration, an optional ultracentrifugation step enables the concentration of the liposomes as illustrated (**Figure 1C**). Based on the absorption and emission properties of the encapsulated dye, the concentration of encapsulated dye is determined with the help of a calibration curve of the free dye (**Figure 1D**). Besides the concentration of the encapsulated dye, it is important to determine the size and homogeneity of the liposomes after preparation. As seen in **Figure 1E**, electron micrographs of liposomes prepared by the underlying method reveal a mostly unilamellar morphology of the liposomal vesicles, containing intravesicular DY-676-COOH either within the quenching concentration range (Lip-Q; 606–846  $\mu$ M DY-676) or at non-quenched dye concentration (Lip-dQ; 25  $\mu$ M DY-676). Furthermore, they reveal a homogenous size distribution of about 120 nm and polydispersity indices far below 1 (**Table 1**). Owing to fluorescence quenching, Lip-Q shows two absorption maxima in aqueous buffer, whereby

one peak is characterized by a shift towards the blue wavelengths. In line with this, the fluorescence emission is very low compared to the free dye (**Figure 2A and B, right**). Freeze-damage of the liposomes results in release of the dye, which gets diluted in the surrounding solution. The blue-shifted absorption peak therefore disappears, resulting in a single absorption peak of Lip-Q. Corresponding to this, an increase in fluorescence intensity of freeze-damaged Lip-Q is seen, which indicates that fluorescence activation of released dye molecules took place. The free dye reveals only a single absorption maximum and high fluorescence intensity which remain at the same level, irrespective of freezing (**Figure 2A and B, left**). This finding suggests that encapsulation of the dye in liposomes, as in Lip-Q would protect the dye from the environment, retain high concentration and the associated fluorescence quenching and if activated by target triggers would enable detection due to increase in fluorescence.

Liposomal probes with the underlying lipid composition reveal a predominant phagocytic uptake which is inhibited by energy depletion. This can be seen via the uptake of Lip-Q by the highly phagocytic murine macrophage cell line J774A.1, and the mildly phagocytic human glioblastoma cell line U-118MG at 37 °C and inhibition at 4 °C (**Figure 3A and B**). The free dye DY-676-COOH reveals uptake in the phagocytic cell lines both at 37 °C and at 4 °C which indicates that the liposomal probe Lip-Q contains no residual free dye in the solution and can only undergo active uptake. Confocal laser scanning microscopic images further substantiate the uptake and activation of Lip-Q in phagocytic cells (**Figure 3C**). Furthermore, the lack of fluorescence in the non-phagocytic human fibrosarcoma cell line, HT-1080 indicates that the uptake of Lip-Q is predominantly by phagocytosis and thus, would be suitable for imaging of inflammation where phagocytic monocytes/macrophages are involved.

Consistent with the phagocytic uptake of liposomes seen in cultured cell lines, and owing to fluorescence quenching intravenous injection of Lip-Q leads to a time-dependent increase in fluorescence intensity of edema in mice models (**Figure 4A, Lip-Q**), with very low background fluorescence. The maximum fluorescence intensity of edema is detected 8-10 hr post injection of Lip-Q. Contrarily, relatively strong NIR-fluorescence of the whole mouse is seen after application of the free DY-676-COOH (**Figure 4A, DY-676-COOH**) or the always-on liposome, Lip-dQ (**Figure 4A, Lip-dQ**). Compared to Lip-Q, rapid perfusion and clearance of the free DY-676-COOH as seen from 0-4 hr post injection, interferes with imaging, so that reliable detection of edema is not possible (**Figure 4A, DY-676-COOH**). Furthermore, the non-quenched liposome, Lip-dQ reveals a maximum fluorescence of edema within 2-4 hr post injection which remains almost constant till 8 hr, then gradually decreases similar to the quenched Lip-Q-based edema fluorescence. Performing semi-quantitative analyses, whereby regions of interest (ROIs) are set for edema versus background, one can make conclusions about the different levels of detection with different probes. According to semi-quantitative analysis of 5 animals per group (probe), edema can be more significantly ( $P = 0.001$ ) detected with Lip-Q than with the free DY-676-COOH or the non-quenched, Lip-dQ (**Figure 4B**).

Imaging organs of mice euthanized 24 hr post injection of probes reveal mild *ex vivo* fluorescence of the liver/gall bladder and kidneys and a very low or no fluorescence of the spleen, lungs and heart (**Figure 5**), which serves as evidence for the elimination of the probes through the hepatobiliary route.



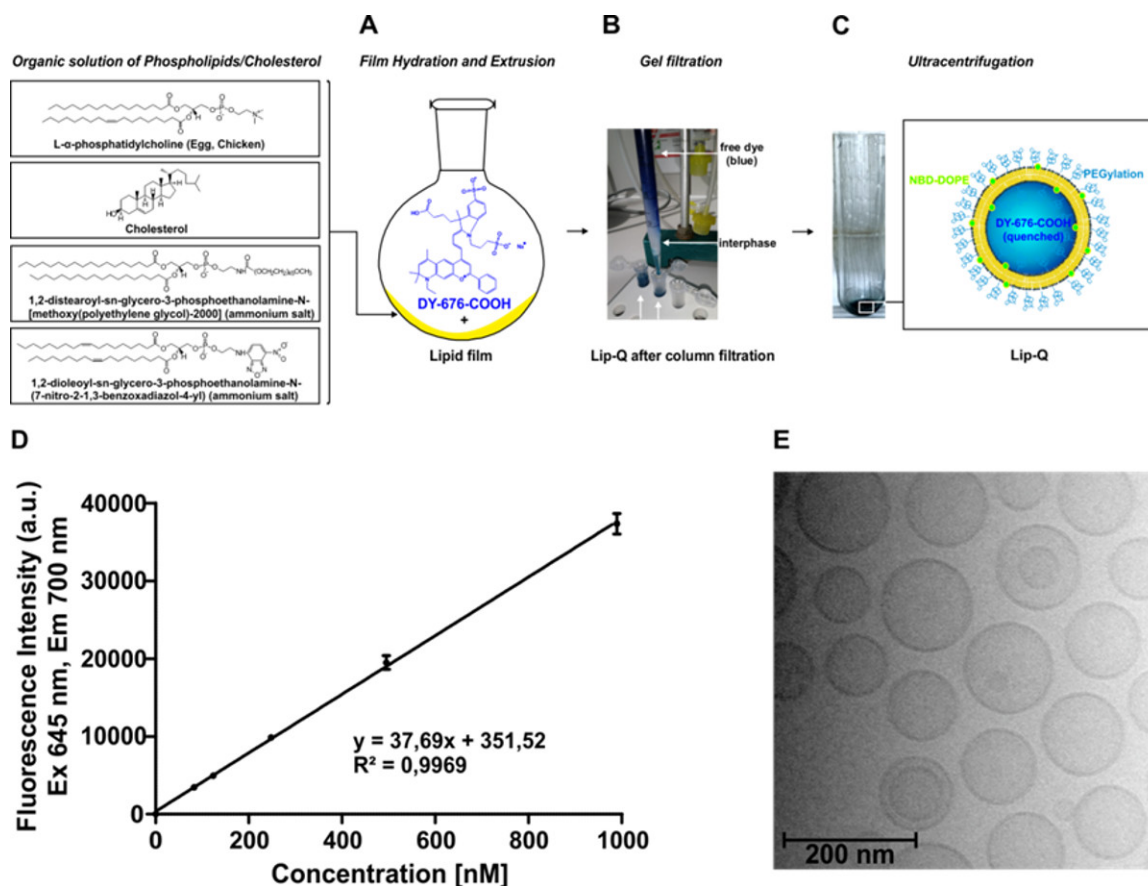


**Figure 1: Preparation of DY-676-COOH-loaded liposomes.** (A-C) Schematic overview of the synthesis steps involved. (A) Setup of the film hydration and extrusion with the near-infrared dye DY-676-COOH. (B) Picture of the self-made gel filtration setup showing the interphase between non-encapsulated (free) dye and liposomes. Liposomes elute first and appear blue-green due to the encapsulated DY-676-COOH (blue) and the incorporated green phospholipid, NBD-DOPE. (C) Representative image of liposome-sediment (Lip-Q) after concentration by ultracentrifugation. (D) Representative calibration curve of DY-676-COOH in 10 mM Tris pH 7.4 (containing 1% Triton X100) used for the quantification of liposomal dye. (E) Cryo-transmission electron micrograph of Lip-Q. [Please click here to view a larger version of the figure.](#)

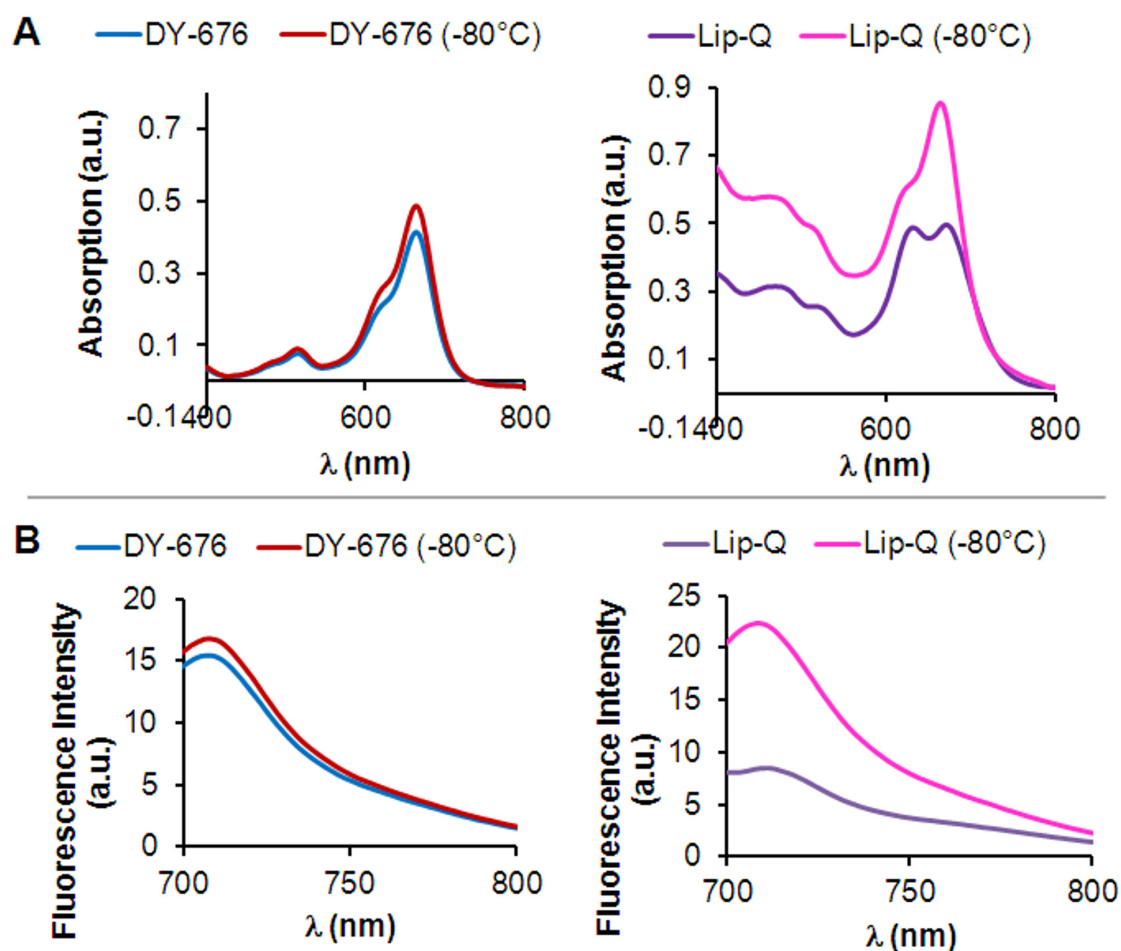


**Figure 2: Physicochemical determination of fluorescence quenching and activation *in vitro*.** (A) Absorption spectra of Lip-Q (right) and free DY-676-COOH (left) measured in 10 mM Tris buffer pH 7.4, before or after freezing at -80 °C. Note the characteristic double peak of Lip-Q compared to free DY-676-COOH and the disappearance of the blue-shifted peak after freeze-damage of Lip-Q. (B) Corresponding fluorescence emission spectra of Lip-Q (right) and free DY-676-COOH (left) measured in 10 mM Tris buffer pH 7.4 before or after freezing at -80 °C.

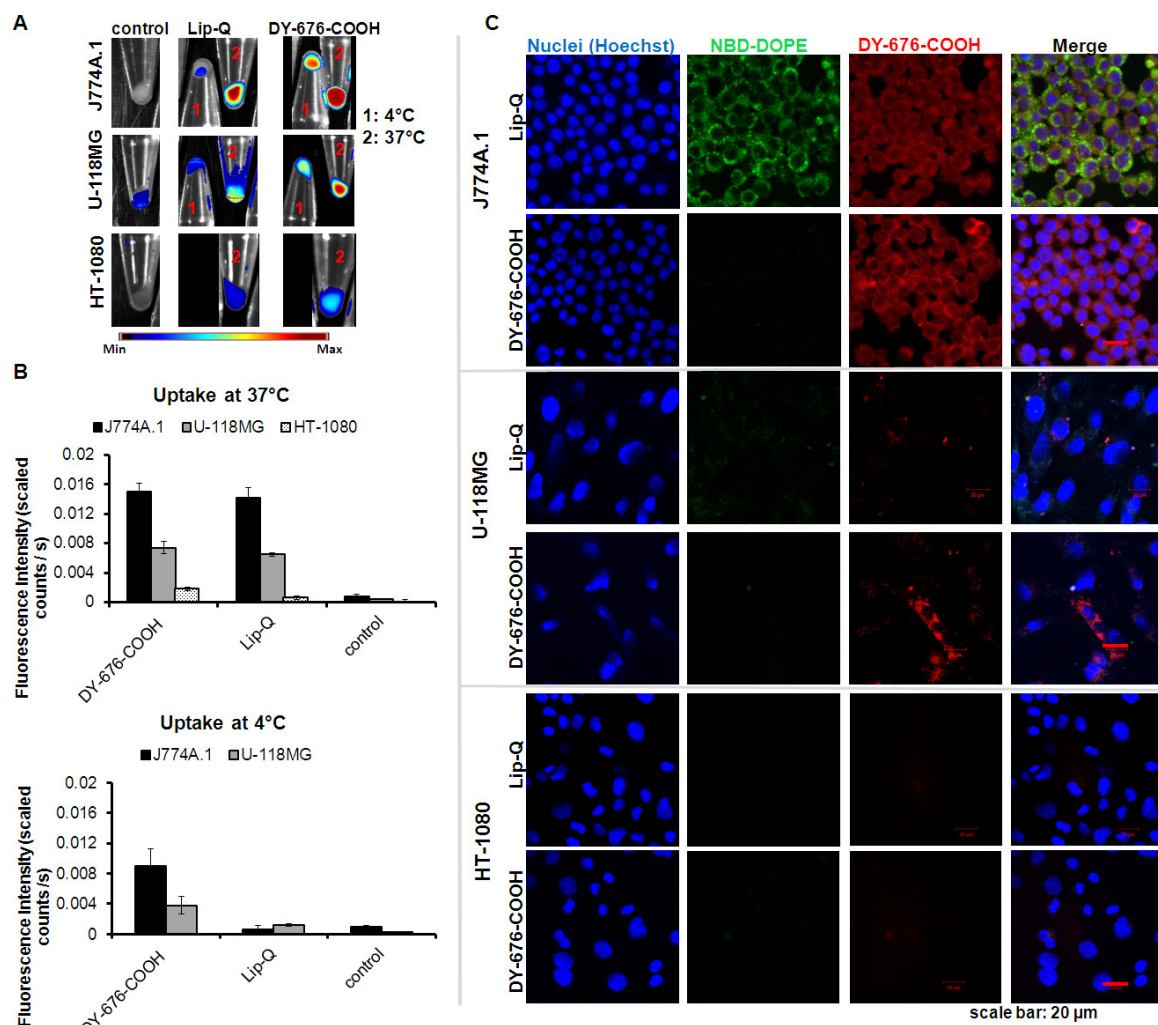


**Figure 3: Cellular uptake and fluorescence activation of liposomes.** The images in (A) were prepared by NIR fluorescence imaging of cell pellets after exposure to the corresponding probes for 24 hr at the indicated temperatures. The HT-1080 cells did not survive the 24 hr incubation periods at 4 °C. The bar diagrams in (B) represent the semi-quantitative levels of fluorescence signals got by assigning ROIs to the cell pellets in A. Each bar denotes the average intensities of  $n = 3$  experiments  $\pm$  SD. Images in (C) were acquired by confocal laser scanning microscopy of cells exposed to probes on culture chamber slides for 24 hr at 37 °C. Note the high level of fluorescence in the high phagocytic murine macrophage cell line J774A.1 and the moderate fluorescence in the mild phagocytic human glioblastoma cell line U-118MG. The non-phagocytic human fibrosarcoma cell line HT-1080 shows no fluorescence of the probes. NBD-DOPE: green fluorescent phospholipid. [Please click here to view a larger version of the figure.](#)



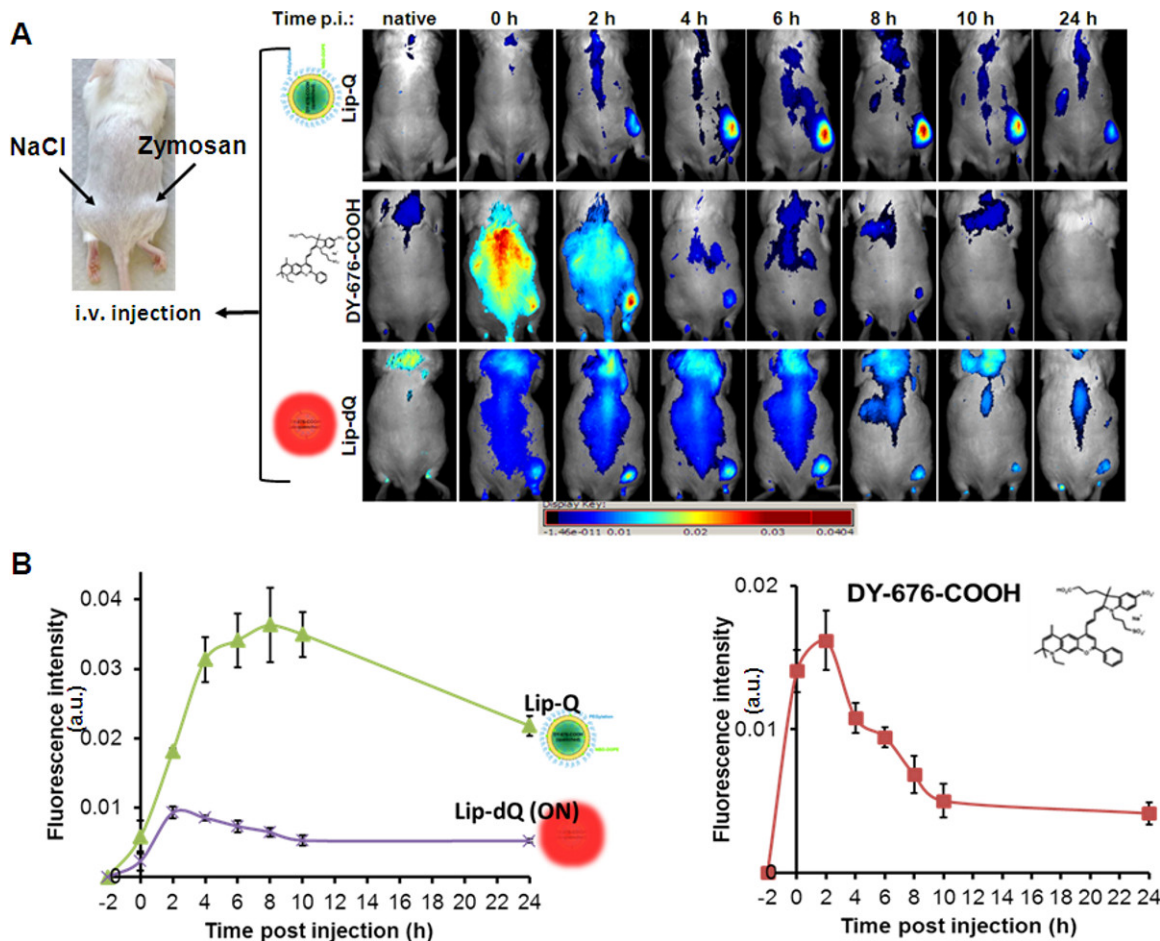


**Figure 4. *In vivo* optical imaging of zymosan-induced edema in mice.** (A) The mouse picture on the left shows the positions of subcutaneously applied zymosan-A (500 µg in 50 µl saline) and the control saline solution (50 µl) on the left flank. Intravenous injection of the indicated probes and whole body NIR fluorescence imaging at the indicated time points reveal gradual, but high increase in fluorescence signals of edema and low background signals of Lip-Q (upper panel) with a maximum fluorescence at 8 hr post injection. The free dye reveals perfusion and rapid clearance within 4 hr post injection (middle panel), whereas Lip-dQ reveals detection of edema with low signal intensities and an overall higher background fluorescence. The graphical presentation in (B) reiterates the observed fluorescence signals of edema detected with each probe compared to the control region (saline) in  $n=5$  animals per group. Each plot represents the mean fluorescence signals of ( $n=5$ )  $\pm$  SEM. With the graphs, the maximum fluorescence signal of edema detected with each probe is easily distinguished (Lip-Q, 8 hr; Lip-dQ 2–4 hr and free DY-676-COOH, 2 hr post injection). There is a significantly ( $P = 0.001$ ) higher fluorescence intensity of edema with Lip-Q versus Lip-dQ at  $t = 0$ –24 hr, and with Lip-Q versus free DY-676-COOH at  $t = 4$ –24 hr. [Please click here to view a larger version of the figure.](#)

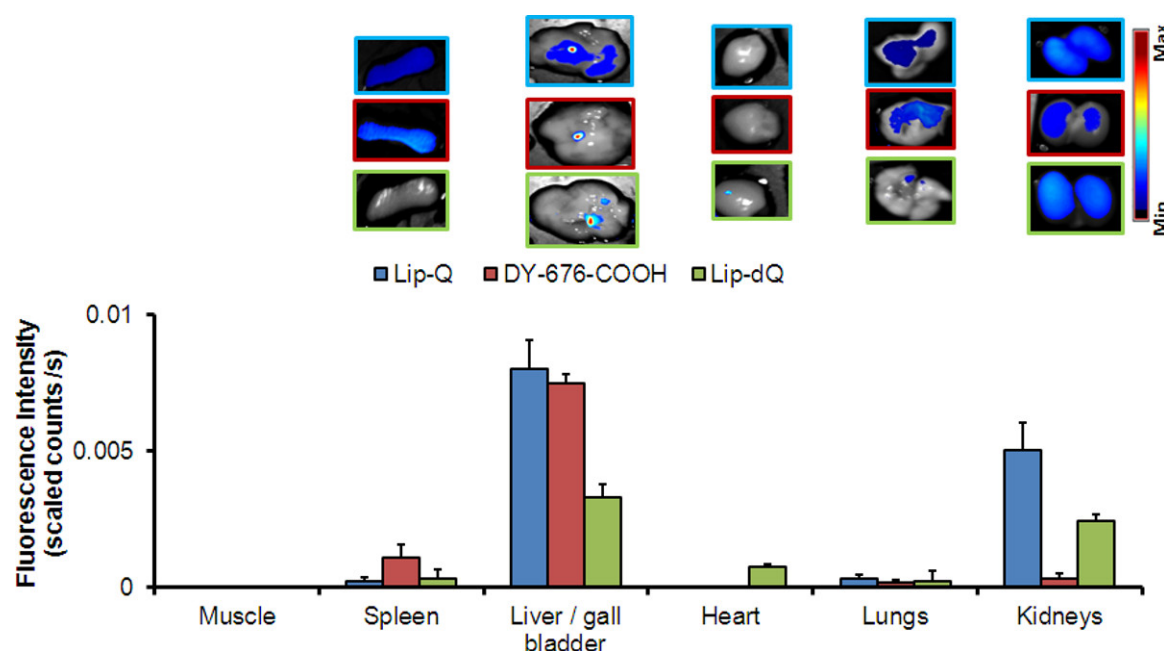


**Figure 5: Bio-optical ex vivo images of organs** from mice 24 hr post probe application, and corresponding semi-quantitative analysis of fluorescence intensities of the organs. Each bar represents the mean of fluorescence intensities ( $n = 4$ )  $\pm$  SEM. [Please click here to view a larger version of the figure.](#)

Liposome formulation	Size [nm]	Polydispersity Index (PI)	Zeta Potential [mV]
Lip-dQ (dequenched)	123.4 $\pm$ 0.6	0.055 $\pm$ 0.02	-10.6 $\pm$ 0.4
Lip-Q (quenched)	118.5 $\pm$ 0.7	0.04 $\pm$ 0.02	-9 $\pm$ 2
Lip-NBD (w/o DY-676-COOH)	123.0 $\pm$ 1.4	0.04 $\pm$ 0.03	-11 $\pm$ 1

**Table 1: Characterization of liposomes by dynamic light scattering.**

## Discussion

Since liposomes can also serve as delivery systems for fluorescent dyes, they enable imaging of target diseases. The encapsulation of high concentrations of fluorescent dyes such as the NIRF dye, DY676-COOH used here, leads to a high level of fluorescence quenching of the entrapped dye. Fluorescence quenching, a phenomenon seen with many fluorophores at high concentration can be exploited in several *in vivo* imaging applications, where a high sensitivity and reliable detection of the target area is demanded. The use of liposomes also provides protection of the dye which is indispensable for *in vivo* applications.

The film hydration and extrusion technique is a widely used method which enables successful preparation of liposomes with different size ranges depending on need, and permits modifications such as encapsulation of a multitude of different substances<sup>25</sup>. Thus, it is suitable for the preparation of liposomes encapsulated with the NIR fluorescent dye, DY-676-COOH for imaging purposes. The method yields liposomes with 600–840  $\mu$ M intravesicular dye concentrations, which are within the quenched concentration of the dye. The LiposoFast-Basic hand extruder used for the homogenization of spontaneously formed vesicle dispersion is suitable for liposome preparation in small lab scale, due to the compatibility of the device, with syringes up to 1 ml volume. For large scale preparations the use of larger high pressure homogenizers which are able to homogenize vesicle dispersions with a capacity of 1,000 L per hour is recommended. The gel filtration (size exclusion) chromatography is a crucial step which ensures separation of the encapsulated liposomal dye from non-encapsulated (free) dye molecules<sup>26</sup>. The length of the gel filtration column is vital for efficient separation of the liposomes from free dye. Thus, it is necessary to prepare a column of at least 28 cm length to successfully separate the liposomes from the free DY-676-COOH used here. Interestingly, this length is two times as long as that used to purify carboxyfluorescein (CF) loaded liposomes from free carboxyfluorescein. The major drawback of gel filtration is a five to six-fold dilution of the purified samples. This can be compensated by ultracentrifugation, if highly concentrated liposomes are needed. During ultracentrifugation the liposomes sediment and the supernatant can be removed easily<sup>27</sup>. Other ways to concentrate liposomes such as by dialysis<sup>28</sup> are more time consuming than ultracentrifugation.

Besides the film hydration and extrusion method, the reversed phase evaporation method<sup>23</sup> as well as the ethanol injection method<sup>24</sup> enable liposome preparation with high encapsulation efficiency for many hydrophilic substances. However, our investigations revealed the film hydration combined with the freeze and thaw cycles to be the most suitable method for a sufficient intraliposomal encapsulation of DY-676-COOH. Increasing the starting DY-676-COOH concentration used for film hydration increases the efficacy and the concentration of the intraliposomal dye, when a fixed lipid concentration of 30 mM is used. Despite this the encapsulation efficacy with the freeze and thaw method is below 10% of the starting dye concentration used, but however is sufficient for encapsulation of the quenching concentration required for imaging. Furthermore, the free dye separated from liposomes by gel filtration can be recycled by desalting and dehydration according to manufacturer instructions,

making re-encapsulation possible and an overall minimal dye loss. The encapsulation of the dye by the underlying protocol has no influence on the size and morphology of the liposomes as seen by the polydispersity indices and the electron micrograph of Lip-Q.

Several simple methods can be used to evaluate the activity of prepared fluorescent liposomes. DY-676-COOH has a high tendency to self-quench at high concentrations<sup>21,29</sup> probably resulting from H-dimer formation and  $\pi$ -stacking interactions between dye molecules. These interactions, which occur due to nearness of the Förster radii of dye molecules at high concentrations, can be annihilated by dilution<sup>30</sup>. Therefore, encapsulation of high concentrations of DY-676-COOH does not only protect the dye from opsonization *in vivo*, but also from the surrounding buffer, thereby maintaining its high concentration and retaining fluorescence quenching which, can be detected as a blue-shifted absorption peak and low fluorescence emission as seen in **Figure 2**. Freezing liposomes gradually at -80 °C leads to formation of ice crystals within the aqueous interior<sup>31</sup> which causes damage to liposomal membrane when rashly thawed at 30 °C. The release, dilution and fluorescence activation of the intra-liposomal DY-676-COOH in buffer after freezing is revealed in a single absorption peak and almost 2.5-fold increase in fluorescence intensity (**Figure 2**), which indicates that Lip-Q thus sequesters a high, quenching concentration of DY-676-COOH and is activatable. Other methods to damage liposomal lipid bilayer such as the use of detergent or organic solvents do not reveal clear-cut differences between the free dye and the liposomal encapsulated dye, since they both influence the spectral properties of many fluorescent dyes<sup>32</sup>. The slow freezing and harsh thawing method reported here therefore serves as a more reliable and promising method to validate the high encapsulation of fluorophores in liposomes and a consequent fluorescence quenching. From the absorption and emission spectra of intact Lip-Q (**Figure 2**), some level of residual fluorescence can be detected. This can result from non-quenched dye monomers within the liposomes and also from electrostatic interaction and influence of encapsulated dye by phospholipid polar head groups<sup>33</sup>.

As can be seen in **Figure 3**, a distinct accumulation of Lip-Q in the highly phagocytic murine macrophage and mild phagocytic human glioblastoma cell line, U-118MG<sup>34</sup>, but not in the non-phagocytic human fibrosarcoma cell line HT-1080, indicates that Lip-Q-based imaging of inflammation would be favorable, since phagocytes are the key players of inflammatory processes. The fact that energy depletion abolishes uptake of Lip-Q but not uptake of the free DY-676-COOH substantiates the specificity of phagocytic uptake of Lip-Q and reveals that Lip-Q remains intact during the experiment, else release of the dye and energy-independent uptake would take place leading to fluorescence detection. Embedding the green fluorescent phospholipid, NBD-DOPE in the liposome bilayer enables microscopic imaging and discrimination between non-degraded from cellular degraded liposomes especially if time-dependent uptake experiments are done as reported earlier<sup>32</sup>. The microscopic images reveal NIR-fluorescence of DY-676-COOH which, correlates with the levels of fluorescence intensities of cell pellets, as determined by semi-quantitative analysis after incubation at 37 °C. In accordance with this, the murine macrophage cell lines show the highest fluorescence, whereas the human glioblastoma reveal lower fluorescence of both DY-676-COOH and NBD-DOPE than the former. As expected the human fibrosarcoma cell line, HT-1080 reveal no fluorescence of either liposomal dyes or the free DY-676-COOH, which strengthens the fact that Lip-Q uptake, is predominantly by phagocytosis.

To investigate the potential of Lip-Q-based phagocytosis-driven *in vivo* imaging of inflammation, several controls were considered. Considering that the free DY-676-COOH can be taken up by phagocytosis, opsonization of Lip-Q may lead to release of the dye, which may be taken up by phagocytes. To avoid this, Lip-Q was prepared with 5 mol% PEGylation. Furthermore, it is necessary to distinguish between uptake due to inflammation-based EPR effect and active uptake and fluorescence activation. To address this, the evaluation and comparison of three different probes, namely the always-on, Lip-dQ, the quenched Lip-Q and the free DY-676-COOH in mice bearing zymosan-induced edema was necessary. Zymosan-A which is prepared from the cell walls of *Saccharomyces cerevisiae* and *Candida albicans* is a natural stimulant of cytokine secretion via the dectin-1 and the toll-like receptor 2/6 (TLR 2/6). Secreted cytokines in turn induce the activation of downstream cascades which result in vascular leakages, thereby easing the intravasation/extravasation of monocytes/macrophages from a splenic reservoir<sup>35</sup> as well as neutrophils, and their migration to inflammation sites (edema)<sup>36-39</sup>. The zymosan-based monocytes/macrophage extravasation and migration process needs only 4.5–6 hr which makes zymosan a strategic tool for studying inflammatory processes<sup>36-39</sup>. Due to the vascular leakages that result during inflammation, intravenously injected probes can either be taken up by monocytes/macrophages (phagocytes) during their migration to the inflammation site or extravasate and be taken up at the edema site (EPR effect)<sup>40</sup>. The use of the non-quenched Lip-dQ reveals an overall stronger background to edema signals than Lip-Q, and a fluorescence increase of edema which reflects the migration of monocytes and macrophages. In effect, the maximum fluorescence of edema is seen already 2–4 hr post application of Lip-dQ and remains almost constant till 8 hr. Opposed to Lip-dQ and Lip-Q, the free DY-676-COOH undergoes rapid perfusion after injection and is cleared within 4 hr, so that distinct imaging of edema is not possible. Interestingly, the use of Lip-Q results in persistent increase in fluorescence intensity of edema and very low background signals. This persistent increase in fluorescence intensities with Lip-Q is attributed to fluorescence activation of the liposomal released dye. Taken together, it can be concluded that the contribution of EPR-effect in Lip-Q based imaging is minimal since Lip-dQ reveal a maximum fluorescence (EPR effect and monocyte migration) at 4 hr post injection. Thus, liposomal encapsulation provides protection and distinct delivery of DY-676-COOH, which in turn enables a more reliable *in vivo* imaging of edema, exclusively after internalization and degradation (fluorescence activation) by phagocytic cells. So far, the use of zymosan-induced hind leg edema to validate the imaging properties of fluorescent liposomes is new. The protocol reported herein can be expanded both by encapsulation of different fluorescent dyes and by imaging the effect of different inhibitory drugs on the induction of inflammation, and therefore represents a useful tool for preparation and characterization of probes suitable for biomedical imaging.

Another crucial step towards defining suitable imaging probes is the verification of their pharmacological properties and elimination routes. The distribution of probes in organs which play vital roles in excretion, such as the liver and kidneys as well as their short retention and suitable elimination from these organs is usually an indication, that the probes will much likely show no adverse effects on the patient. In accordance with this, the organs of mice prepared 24 hr post injection of Lip-Q or the free DY-676-COOH reveal only mild fluorescence of the liver/gall bladder and the kidneys, which signifies a preferred elimination of the liposomal fluorophore through the hepatobiliary route. The short accommodation of the probes in these organs and their efficient elimination is substantiated by a 7-fold higher fluorescence signals of organs prepared 6 hr post injection of Lip-Q or the free DY-676-COOH<sup>32</sup>. These observations are in accordance with the elimination of liposomes<sup>41</sup> and backs up the importance of including biodistribution studies when characterizing probes. Although adverse side effects, such as skin irritations and complement activation<sup>42,43</sup> have been reported for liposomal formulations used in clinical applications, such effects were not detected with the underlying liposomes. Furthermore, observation of immune deficient mice for two weeks after probe injection led to complete clearance of the probes from the mice organs (not shown).

## Disclosures

The authors have nothing to disclose.

## Acknowledgements

This work was supported by the *Deutsche Forschungsgemeinschaft* grants HI-698/10-1 and RU-1652/1-1. We thank Doreen May for excellent technical assistance and the company DYOMICS GmbH, Jena for their kind support.

## References

1. Buse, J., & El-Aneed, A. Properties, engineering and applications of lipid-based nanoparticle drug-delivery systems: current research and advances. *Nanomedicine (Lond)*. **5**, 1237-1260, doi:10.2217/nnm.10.107 (2010).
2. Lim, S. B., Banerjee, A., & Onyuksel, H. Improvement of drug safety by the use of lipid-based nanocarriers. *Journal of controlled release : official journal of the Controlled Release Society*. **163**, 34-45, doi:10.1016/j.jconrel.2012.06.002 (2012).
3. Cabanes, A. *et al.* Enhancement of antitumor activity of polyethylene glycol-coated liposomal doxorubicin with soluble and liposomal interleukin 2. *Clinical cancer research : an official journal of the American Association for Cancer Research*. **5**, 687-693 (1999).
4. Gabizon, A., Shmeeda, H., & Grenader, T. Pharmacological basis of pegylated liposomal doxorubicin: impact on cancer therapy. *European journal of pharmaceutical sciences : official journal of the European Federation for Pharmaceutical Sciences*. **45**, 388-398, doi:10.1016/j.ejps.2011.09.006 (2012).
5. Balasubramanian, S. V., Bruenn, J., & Straubinger, R. M. Liposomes as formulation excipients for protein pharmaceuticals: a model protein study. *Pharmaceutical research*. **17**, 344-350 (2000).
6. Meyer, J., Whitcomb, L., & Collins, D. Efficient encapsulation of proteins within liposomes for slow release in vivo. *Biochemical and biophysical research communications*. **199**, 433-438, doi:10.1006/bbrc.1994.1247 (1994).
7. Mayer, L. D., Hope, M. J., & Cullis, P. R. Vesicles of variable sizes produced by a rapid extrusion procedure. *Biochimica et biophysica acta*. **858**, 161-168 (1986).
8. Mayer, L. D., Bally, M. B., Hope, M. J., & Cullis, P. R. Techniques for encapsulating bioactive agents into liposomes. *Chemistry and physics of lipids*. **40**, 333-345 (1986).
9. Walde, P., & Ichikawa, S. Enzymes inside lipid vesicles: preparation, reactivity and applications. *Biomolecular engineering*. **18**, 143-177 (2001).
10. Weissleder, R., & Ntziachristos, V. Shedding light onto live molecular targets. *Nature medicine*. **9**, 123-128, doi:10.1038/nm0103-123 (2003).
11. Licha, K., Riefke, B., Ebert, B., & Grotzinger, C. Cyanine dyes as contrast agents in biomedical optical imaging. *Academic radiology*. **9 Suppl 2**, S320-322 (2002).
12. Pauli, J. *et al.* Novel fluorophores as building blocks for optical probes for in vivo near infrared fluorescence (NIRF) imaging. *Journal of fluorescence*. **20**, 681-693, doi:10.1007/s10895-010-0603-7 (2010).
13. Holzer, W. *et al.* Photostability and thermal stability of indocyanine green. *Journal of photochemistry and photobiology. B, Biology*. **47**, 155-164 (1998).
14. Gandorfer, A., Haritoglou, C., & Kampik, A. Retinal damage from indocyanine green in experimental macular surgery. *Investigative ophthalmology & visual science*. **44**, 316-323 (2003).
15. Saxena, V., Sadoqi, M., & Shao, J. Degradation kinetics of indocyanine green in aqueous solution. *Journal of pharmaceutical sciences*. **92**, 2090-2097, doi:10.1002/jps.10470 (2003).
16. Kodjikian, L. *et al.* Toxic effects of indocyanine green, infracyanine green, and trypan blue on the human retinal pigmented epithelium. *Graefes's archive for clinical and experimental ophthalmology = Albrecht von Graefes Archiv fur klinische und experimentelle Ophthalmologie*. **243**, 917-925, doi:10.1007/s00417-004-1121-6 (2005).
17. Sevcik-Muraca, E. M., Houston, J. P., & Gurfinkel, M. Fluorescence-enhanced, near infrared diagnostic imaging with contrast agents. *Current opinion in chemical biology*. **6**, 642-650 (2002).
18. Bremer, C., Ntziachristos, V., & Weissleder, R. Optical-based molecular imaging: contrast agents and potential medical applications. *European radiology*. **13**, 231-243, doi:10.1007/s00330-002-1610-0 (2003).
19. Hilderbrand, S. A., Kelly, K. A., Weissleder, R., & Tung, C. H. Monofunctional near-infrared fluorochromes for imaging applications. *Bioconjugate chemistry*. **16**, 1275-1281, doi:10.1021/bc0501799 (2005).
20. Langhals, H. *et al.* Cyanine dyes as optical contrast agents for ophthalmological surgery. *Journal of medicinal chemistry*. **54**, 3903-3925, doi:10.1021/jm2001986 (2011).
21. Pauli, J. *et al.* An in vitro characterization study of new near infrared dyes for molecular imaging. *European journal of medicinal chemistry*. **44**, 3496-3503, doi:10.1016/j.ejmech.2009.01.019 (2009).
22. Ogawa, M., Kosaka, N., Choyke, P. L., & Kobayashi, H. H-type dimer formation of fluorophores: a mechanism for activatable, in vivo optical molecular imaging. *ACS chemical biology*. **4**, 535-546, doi:10.1021/cb900089j (2009).
23. Szoka, F., Jr., & Papahadjopoulos, D. Procedure for preparation of liposomes with large internal aqueous space and high capture by reverse-phase evaporation. *Proc.Natl.Acad.Sci.U.S.A.* **75**, 4194-4198 (1978).
24. Batzri, S., & Korn, E. D. Single bilayer liposomes prepared without sonication. *Biochimica et biophysica acta*. **298**, 1015-1019 (1973).
25. Fahr, A., van Hoogevest, P., May, S., Bergstrand, N., & ML, S. L. Transfer of lipophilic drugs between liposomal membranes and biological interfaces: consequences for drug delivery. *European journal of pharmaceutical sciences : official journal of the European Federation for Pharmaceutical Sciences*. **26**, 251-265, doi:10.1016/j.ejps.2005.05.012 (2005).
26. New, R. C. *Liposomes a practical approach*. IRL Press at Oxford University Press, (1990).
27. Barenholz, Y. *et al.* A simple method for the preparation of homogeneous phospholipid vesicles. *Biochemistry*. **16**, 2806-2810 (1977).
28. Schwendener, R. A. The preparation of large volumes of homogeneous, sterile liposomes containing various lipophilic cytostatic drugs by the use of a capillary dialyzer. *Cancer drug delivery*. **3**, 123-129 (1986).



29. Pauli, J. *et al.* Suitable labels for molecular imaging--influence of dye structure and hydrophilicity on the spectroscopic properties of IgG conjugates. *Bioconjugate chemistry*. **22**, 1298-1308, doi:10.1021/bc1004763 (2011).
30. Wu, P., & Brand, L. Resonance energy transfer: methods and applications. *Analytical biochemistry*. **218**, 1-13 (1994).
31. Stark, B., Pabst, G., & Prassl, R. Long-term stability of sterically stabilized liposomes by freezing and freeze-drying: Effects of cryoprotectants on structure. *European journal of pharmaceutical sciences : official journal of the European Federation for Pharmaceutical Sciences*. **41**, 546-555, doi:10.1016/j.ejps.2010.08.010 (2010).
32. Tansi, F. L. *et al.* Liposomal encapsulation of a near-infrared fluorophore enhances fluorescence quenching and reliable whole body optical imaging upon activation in vivo. *Small*. **9**, 3659-3669, doi:10.1002/smll.201203211 (2013).
33. Chen, R. F., & Knutson, J. R. Mechanism of fluorescence concentration quenching of carboxyfluorescein in liposomes: energy transfer to nonfluorescent dimers. *Analytical biochemistry*. **172**, 61-77 (1988).
34. Windler-Hart, S. L., Chen, K. Y., & Chenn, A. A cell behavior screen: identification, sorting, and enrichment of cells based on motility. *BMC cell biology*. **6**, 14, doi:10.1186/1471-2121-6-14 (2005).
35. Swirski, F. K. *et al.* Identification of splenic reservoir monocytes and their deployment to inflammatory sites. *Science*. **325**, 612-616, doi:10.1126/science.1175202 (2009).
36. Erdo, F., Torok, K., Aranyi, P., & Szekely, J. I. A new assay for antiphlogistic activity: zymosan-induced mouse ear inflammation. *Agents and actions*. **39**, 137-142 (1993).
37. Ajuebor, M. N. *et al.* Endogenous monocyte chemoattractant protein-1 recruits monocytes in the zymosan peritonitis model. *Journal of leukocyte biology*. **63**, 108-116 (1998).
38. Ajuebor, M. N., Das, A. M., Virag, L., Szabo, C., & Perretti, M. Regulation of macrophage inflammatory protein-1 alpha expression and function by endogenous interleukin-10 in a model of acute inflammation. *Biochemical and biophysical research communications*. **255**, 279-282, doi:10.1006/bbrc.1999.0196 (1999).
39. Ajuebor, M. N. *et al.* Role of resident peritoneal macrophages and mast cells in chemokine production and neutrophil migration in acute inflammation: evidence for an inhibitory loop involving endogenous IL-10. *J Immunol*. **162**, 1685-1691 (1999).
40. Binstadt, B. A. *et al.* Particularities of the vasculature can promote the organ specificity of autoimmune attack. *Nature immunology*. **7**, 284-292, doi:10.1038/ni1306 (2006).
41. Ishida, T., Harashima, H., & Kiwada, H. Liposome clearance. *Bioscience reports*. **22**, 197-224 (2002).
42. Dobrovolskaia, M. A., & McNeil, S. E. Understanding the correlation between in vitro and in vivo immunotoxicity tests for nanomedicines. *Journal of controlled release : official journal of the Controlled Release Society*. **172**, 456-466, doi:10.1016/j.jconrel.2013.05.025 (2013).
43. Szebeni, J. *et al.* Prevention of infusion reactions to PEGylated liposomal doxorubicin via tachyphylaxis induction by placebo vesicles: a porcine model. *Journal of controlled release : official journal of the Controlled Release Society*. **160**, 382-387, doi:10.1016/j.jconrel.2012.02.029 (2012).